Supercapacitors

DOI: 10.1002/anie.201405325

Fabrication of Ultralong Hybrid Microfibers from Nanosheets of Reduced Graphene Oxide and Transition-Metal Dichalcogenides and their Application as Supercapacitors**

Gengzhi Sun, Juqing Liu, Xiao Zhang, Xuewan Wang, Hai Li, Yang Yu, Wei Huang, Hua Zhang, and Peng Chen**

Abstract: *Two-dimensional materials have attracted increasing research interest owing to their unique electronic, physical, optical, and mechanical properties. We thus developed a general strategy for the fabrication of ultralong hybrid microfibers from a mixture of reduced graphene oxide and transition-metal dichalcogenides (TMDs), including MoS_2, TiS_2, TaS_2, and $NbSe_2$. Furthermore, we prepared fiber-based solid-state supercapacitors as a proof-of-concept application. The performance of thus-prepared supercapacitors was greatly improved by the introduction of the TMDs.*

In recent years, fiber-based devices have attracted great attention because of their potential applications in portable and wearable electronics.[1] So far, fiber-based electric generators,[2] non-volatile memory,[3] transistors,[4] sensors,[5] actuators,[6] solar cells,[7] Li-ion batteries,[8] and supercapacitor[9] that could be woven into smart textiles, have been reported. Because of their high conductivity and availability, metallic fibers were first employed in the aforementioned applications.[7] However, their tendency to be oxidized under ambient conditions, poor wearing comfort, and their high weight limit their applications in wearable electronics.[9,10] Alternatively, carbon nanotube (CNT) fibers spun from vertically aligned CNT arrays exhibit excellent flexibility,[11] good mechanical strength, and electrical conductivity.[12] However, the fabrication of CNT fibers is technically nontrivial, and CNTs, particularly in the densely packed form, are chemically inert. Reduced graphene oxide (rGO), which can be synthesized by low-cost, scalable solution processes and equipped with abundant functional groups on its surface, is a unique alternative for the fabrication of fibers. So far, a few studies have demonstrated the fabrication and applications of rGO fibers.[13]

In the past decade, the two-dimensional (2D) single atomic layer material graphene has attracted increasing research interest, owing to its unique electronic, physical, chemical, optical, and mechanical properties.[14] Besides graphene, the interesting properties of 2D nanosheets of transition-metal dichalcogenides (TMDs) led to many applications.[15] Herein, we present a general strategy for the fabrication of ultralong hybrid microfibers from the nanosheets of rGO and TMDs (e.g. MoS_2, TiS_2, TaS_2, and $NbSe_2$). As a proof-of-concept application, the hybrid-fiber-based supercapacitors were prepared and studied.

The liquid crystalline behavior of highly concentrated aqueous suspension of graphene oxide (GO) nanosheets enables the assembly of GO nanosheets into macroscopic fibers using a simple wet-spinning method.[16] The fiber-spinning process is schematically illustrated in Figure 1 A. After the preparation of GO nanosheets by a modified Hummers method,[17] AFM image showed the height of GO to be approximately 1 nm (Figure S1), thus indicating that GO was obtained in a single atomic layer.[17,18] The aqueous GO suspension (20 mg mL^{-1}) was then injected into an ethanolic KOH solution by a syringe. A polytetrafluoroethylene (PTFE) rod was used to collect the GO fibers from the ethanolic KOH coagulation bath. During the spinning process, several parameters could be tuned to control the formation of GO fibers, including the injection rate of the GO suspension into the bath, the fiber collection rate, and the concentration of KOH in ethanol. In this study, an injection rate of 5 mL min^{-1}, a collection rate of 55 rpm, and a saturated ethanolic KOH solution were used. The GO fiber could be spun-out continuously without a limitation to its length. Figure 1 B shows a single GO fiber around a PTFE rod.

[*] Dr. G. Z. Sun,[+] X. W. Wang, Y. Yu, Prof. P. Chen
School of Chemical and Biomedical Engineering
Nanyang Technological University
70 Nanyang Drive, Singapore 637457 (Singapore)
E-mail: chenpeng@ntu.edu.sg
Dr. J. Q. Liu,[+] X. Zhang, Dr. H. Li, Prof. H. Zhang
School of Materials Science and Engineering
Nanyang Technological University
50 Nanyang Avenue, Singapore 639798 (Singapore)
E-mail: hzhang@ntu.edu.sg
Homepage: http://www.ntu.edu.sg/home/hzhang/
Dr. J. Q. Liu,[+] Prof. W. Huang
Singapore-Jiangsu Joint Research Center for Organic/Bio-Electronics and Information Displays & Institute of Advanced Materials (IAM), Nanjing Tech University
Nanjing 211816 (China)
[+] These authors contributed equally to this work.

[**] This work was supported by a SERC Grant (no 102 170 0142) from the Agency for Science, Technology and Research (A*STAR, Singapore), AcRF Tier 2 (MOE2011-T2-2-010, MOE2013-T2-1-034), AcRF Tier 1 (RG 61/12, RGT18/13, and RG5/13), and a start-up grant (M4080865.070.706022) in Singapore, and NNSF (61376088, 51302134) in China. This research was also supported by NTU-HUJ-BGU Nanomaterials for Energy and Water Management Programme under the Campus for Research Excellence and Technological Enterprise (CREATE), that is supported by the National Research Foundation, Prime Minister's Office, Singapore.

Supporting information for this article is available on the WWW under http://dx.doi.org/10.1002/anie.201405325.

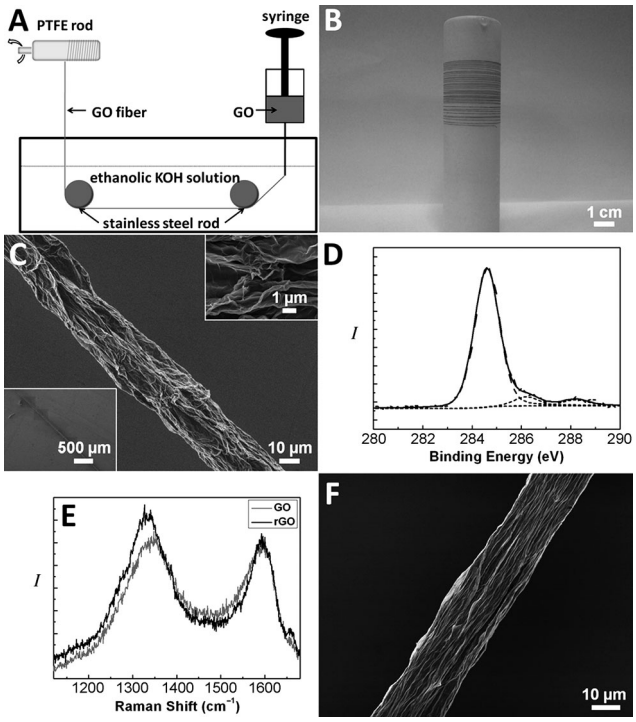

Figure 1. A) Schematic illustration of the fabrication of GO fibers. B) Photograph of a single as-spun GO fiber around a PTFE rod. C) Typical SEM image of an rGO fiber. Insets: Low (bottom left corner) and high (top right corner) magnification of the SEM image of the rGO fiber. D) XPS spectrum of rGO fibers. E) Raman spectra of GO and rGO fibers. F) SEM image of rGO–MoS_2 hybrid fiber (2.2 wt% of MoS_2).

After the GO fiber was washed several times with ethanol, it was chemically reduced by hydroiodic acid (HI), which, compared with the commonly used hydrazine, is a safer, more convenient, and effective reducing agent.[19] As shown in the scanning electron microscopy (SEM) images (Figure 1C), the obtained rGO fiber is composed of aligned rGO sheets with numerous edges and wrinkles, which are believed to be more electrochemically active.[20] The reduction of GO was confirmed by X-ray photoelectron spectroscopy (XPS), which indicates that the C–O and C=O peaks (at 286.8 and 288.5 eV) were significantly reduced (Figure 1D) compared to that of the GO fiber (Figure S2). This result is consistent with the observation in the Raman spectrum, that is, the D (1336 cm^{-1}) and G (1594 cm^{-1}) bands were slightly sharpened and their intensity ratio (I_D/I_G) was increased after reduction (Figure 1E). The conductivity of as-prepared rGO fibers is approximately 200 $S\,m^{-1}$.

The MoS_2 nanosheets were prepared by the electrochemical intercalation method, which was developed in one of our previous studies.[21] After the exfoliation, the as-prepared single-layer MoS_2 nanosheets were resuspended in deionized water and ultrasonicated prior to use. In order to fabricate the rGO–MoS_2 hybrid fiber, GO (20 $mg\,mL^{-1}$, 5 mL) and MoS_2 (0.2 $mg\,mL^{-1}$, 11 mL) dispersions were well-mixed with a vortex mixer. After centrifugation, the gel-like suspension at the bottom was collected and used for the fiber spinning. As shown in the SEM image, the obtained hybrid fiber showed a morphology that was similar to that of an rGO fiber (Figure 1F). Energy dispersive spectroscopy (EDS) confirmed the incorporation of MoS_2 in the hybrid fiber (Figure S3). The conductivity of this hybrid fiber with 2.2 wt% of MoS_2 was approximately 175 $S\,m^{-1}$, which is similar to that of the rGO fiber (around 200 $S\,m^{-1}$).

Owing to their unique optoelectronic properties, TMD materials (particularly MoS_2), when coupled with conducting materials, have various potential applications, such as in hydrogen evolution,[22] Li-ion batteries,[23] solar cells,[24] and supercapacitors.[25] As a proof-of-concept application, the rGO–MoS_2 hybrid fiber was used in a solid-state fiber-based supercapacitor. Figure 2A schematically shows how this kind of supercapacitor was fabricated. After the hybrid fibers were coated with a gel electrolyte consisting of polyvinyl alcohol (PVA) and H_2SO_4, two of the fibers were slightly twisted to produce a fiber-based supercapacitor. For the electrochemical measurements, Ag paste was applied at both ends of the twisted fiber. A photograph of such a supercapacitor is shown in Figure 2B. The SEM image shows that the two fibers are slightly interwoven (Figure 2C) and that their surface is covered by the PVA-H_2SO_4 gel electrolyte (Figure 2D).

The capacitive performance of bare rGO fibers and rGO–MoS_2 hybrid fiber based devices was tested in a two-electrode configuration. The volumetric capacitance (at a discharge current of 1 μA) of the rGO–MoS_2 hybrid fiber based device depended on the ratio of MoS_2 (Figure 3A). It increased from 1.5 $F\,cm^{-3}$ for the bare rGO fiber to 16.5 $F\,cm^{-3}$ for the hybrid

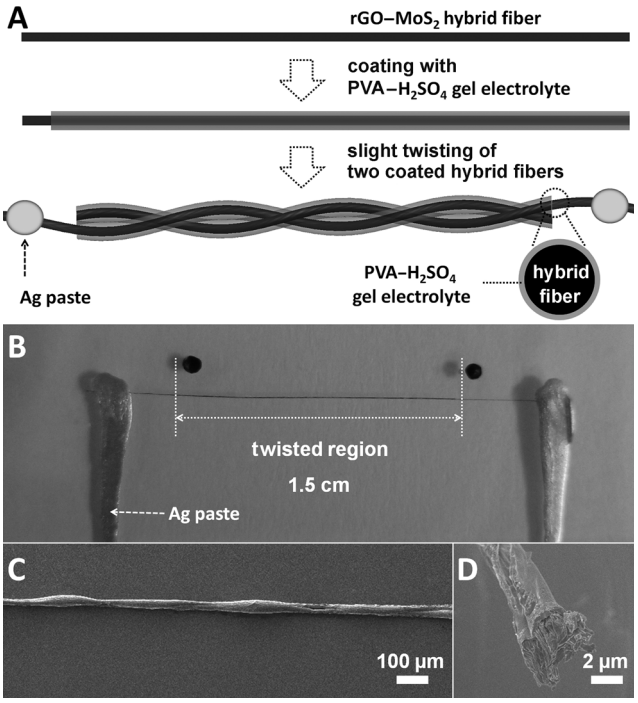

Figure 2. A) Schematic illustration of the fabrication of an rGO–MoS_2 hybrid fiber based supercapacitor. B) Photograph and C) SEM image of an as-fabricated rGO–MoS_2 fiber based supercapacitor. The two black pins in (B) are used as markers to indicate the twisted region. D) Cross-sectional SEM image of an rGO–MoS_2 hybrid fiber coated with the PVA–H_2SO_4 gel electrolyte.

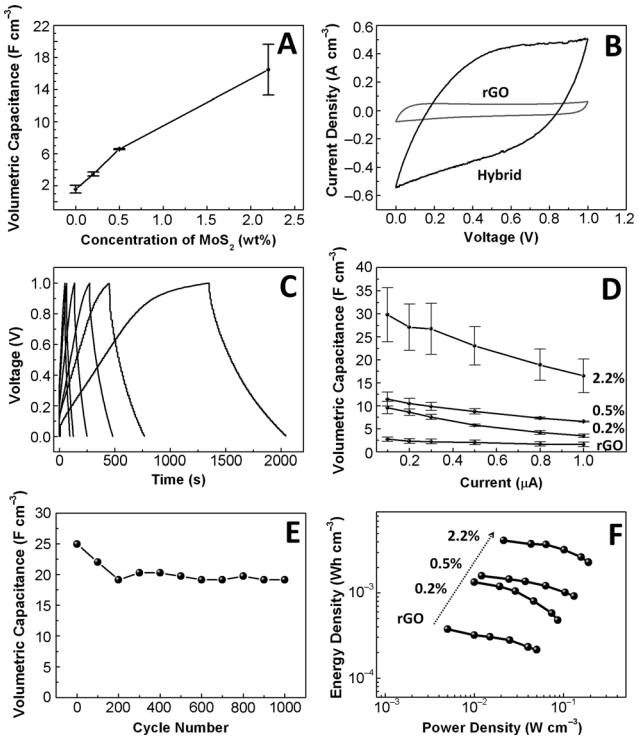

Figure 3. A) MoS_2-concentration-dependent volumetric capacitance of the rGO–MoS_2 hybrid fiber based supercapacitor. B) Cyclic voltammograms of supercapacitors based on bare rGO fibers and rGO–MoS_2 (2.2 wt%) hybrid fibers. C) Typical charge–discharge curves with discharge currents from 0.1 to 1.0 μA. D) Current-dependent capacitive performance of a bare rGO fiber and rGO–MoS_2 hybrid fibers with different MoS_2 concentration (0.2, 0.5, 2.2 wt%). E) Cycling stability of an rGO–MoS_2 (2.2 wt%) hybrid fiber based supercapacitor. F) Relation between power density and energy density of the rGO–MoS_2 fiber based supercapacitor. The error bars in (A) and (D) indicate the standard deviation ($n=3$).

fiber with 2.2 wt% of MoS_2. Note that once the concentration of MoS_2 exceeded 2.2 wt%, aggregation occurred in the GO-MoS_2 gel-like mixture formed after centrifugation. Figure 3B shows the cyclic voltammograms (CV) of a bare rGO fiber based device and a rGO–MoS_2 (2.2 wt%) hybrid fiber based device at a scan rate of 10 mV s^{-1}. The CV curve of the rGO fiber based supercapacitor has a slightly distorted rectangular shape, which indicates that the typical electric double-layer capacitance (EDLC) behavior dominated the charge–discharge process.[26] In contrast, the rGO–MoS_2 (2.2 wt%) hybrid fiber based supercapacitor has a much higher current density and a distorted CV curve, owing to the pseudocapacitive contribution from MoS_2.[25,27] Figure 3C displays the galvanostatic charge–discharge curves of the rGO–MoS_2 (2.2 wt%) hybrid fiber based supercapacitor at charge–discharge currents ranging from 0.1 to 1 μA. Figure 3D compares the specific capacitances at various currents of supercapacitors based on rGO fibers and rGO–MoS_2 hybrid fibers at different ratios of MoS_2. The average volumetric specific capacitance of the rGO–MoS_2 (2.2 wt%) hybrid fiber based device is around 30 F cm^{-3} (at a current of 0.1 μA). This value is higher than that of fiber-based solid supercapacitors consisting of ZnO nanowires/graphene films (0.36 F cm^{-3})[28] and MnO_2/CNT composite fibers (4.5 F cm^{-3}),[29] but is comparable to the value of supercapacitors based on coaxial CNT fibers (32 F cm^{-3}).[30]

The cyclic stability of the rGO–MoS_2 (2.2 wt%) hybrid fiber based supercapacitor was evaluated next. The specific capacitance decayed slightly in the first 200 cycles, but remained relatively stable up to 1000 cycles (Figure 3E). The energy density and power density can be calculated by $E=1/2\,CV^2$ and $P=E/t_{\text{discharge}}$, where C, V, and $t_{\text{discharge}}$ are the capacitance, working voltage, and discharging time, respectively. E and P depend on the conductivity of the electrodes, the diffusion kinetics of ions, and the kinetics of the pseudo capacitance of MoS_2. As observed at a given power density, the MoS_2 loading leads to a large improvement in energy density in a concentration-dependent manner (Figure 3F). By employing the same protocol, other TMD materials (TiS_2, TaS_2, and $NbSe_2$) were successfully used to fabricate rGO–TMD hybrid fibers. Their capacitive performance was also tested, which is improved compared to that of the bare rGO fiber (Figure S4).

The bare rGO fiber exhibited a small capacitance originating from the EDLC,[26a] as ions can hardly penetrate into the interior of the fiber because of the restacking of the rGO sheets.[31] The strong coupling in hybrid films between graphene and adopted elements, such as CNT and titanate nanosheets, has been reported.[32] Therefore, the improved performance of the rGO–MoS_2 hybrid fibers introduced in this study could be attributed to three main reasons. First, the intercalated TMD sheets serve as spacers to alleviate restacking between rGO sheets.[31] Second, the electrochemically active TMDs lead to large pseudo-capacitance.[25] Finally, the interconnected rGO network provides EDLC and also serves as a highly conductive material for charge transfer and transport.[33]

In summary, a general and facile strategy to fabricate ultralong hybrid microfibers from rGO and 2D TMD nanomaterials has been developed. As a proof-of-concept application, solid-state supercapacitors based on rGO–TMD hybrid fibers were fabricated, showing an improved performance compared to devices based on bare rGO fibers.

Experimental Section

GO sheets were prepared following the protocol described in our previous study.[17] The obtained aqueous GO suspension was centrifuged at 10000 rpm for 30 min, and the gel-like suspension at the bottom was collected for GO fiber spinning. The saturated ethanolic KOH solution was used as coagulation bath. The GO suspension (20 mg mL^{-1}) was injected into an ethanolic KOH solution by a syringe at a rate of 5 mL min^{-1}. A PTFE rod was used to collect the GO fiber from the ethanolic KOH bath with a collection rate of 55 rpm. After washing several times with ethanol, the GO fiber was chemically reduced with HI to produce rGO fibers.[19] The transition-metal dichalcogenides (TMDs, such as MoS_2, TiS_2, TaS_2, and $NbSe_2$) were synthesized using the electrochemical intercalation method.[21] The suspension of exfoliated TMD nanosheets was centrifuged and washed several times with water prior to use. Hybrid fibers were fabricated using a wet-spinning process as described in text. Briefly, a certain amount of the as-prepared aqueous dispersion of TMD nanosheets was mixed with GO with a vortex mixer. After centrifugation, the gel-like suspension at the bottom was collected and used

for the spinning of hybrid fiber. The experimental conditions for fabrication of rGO–TMD hybrid fibers are the same as those used for preparation of rGO fibers.

In order to demonstrate their potential application, the hybrid fibers were first coated with PVA-H_2SO_4 gel electrolyte and then slightly twisted to produce a fiber-based supercapacitor. The PVA-H_2SO_4 gel electrolyte was prepared by mixing an aqueous solution of H_2SO_4 (1M) with PVA powder (1 g), and then heating the resulting mixture at 90 °C with vigorous stirring to obtain a homogeneous gel-like suspension. For electrochemical measurements, Ag paste was applied at both ends of the twisted fiber. The capacitive performance was tested in a two-electrode configuration. The maximum charge–discharge current that was used (1 μA) corresponds to the current density of around 1 A cm^{-3}.

Received: May 15, 2014
Published online: August 11, 2014

Keywords: graphene · hybrid fibers · nanotechnology · supercapacitors · transition-metal dichalcogenides

[1] a) T. Chen, L. B. Qiu, Z. B. Yang, H. S. Peng, *Chem. Soc. Rev.* **2013**, *42*, 5031 – 5041; b) D. C. Zou, Z. B. Lv, X. Cai, S. C. Hou, *Nano Energy* **2012**, *1*, 273 – 281.

[2] Y. Qin, X. D. Wang, Z. L. Wang, *Nature* **2008**, *451*, 809 – 813.

[3] G. Z. Sun, J. Q. Liu, L. X. Zheng, W. Huang, H. Zhang, *Angew. Chem. Int. Ed.* **2013**, *52*, 13351 – 13355; *Angew. Chem.* **2013**, *125*, 13593 – 13597.

[4] M. Hamedi, L. Herlogsson, X. Crispin, R. Marcilla, M. Berggren, O. Inganas, *Adv. Mater.* **2009**, *21*, 573 – 577.

[5] Y. Liu, G. Z. Sun, C. B. Jiang, X. T. Zheng, L. X. Zheng, C. M. Li, *Microchim. Acta* **2014**, *181*, 63 – 70.

[6] J. Foroughi, G. M. Spinks, G. G. Wallace, J. Oh, M. E. Kozlov, S. L. Fang, T. Mirfakhrai, J. D. W. Madden, M. K. Shin, S. J. Kim, R. H. Baughman, *Science* **2011**, *334*, 494 – 497.

[7] M. R. Lee, R. D. Eckert, K. Forberich, G. Dennler, C. J. Brabec, R. A. Gaudiana, *Science* **2009**, *324*, 232 – 235.

[8] Y. H. Lee, J. S. Kim, J. Noh, I. Lee, H. J. Kim, S. Choi, J. Seo, S. Jeon, T. S. Kim, J. Y. Lee, J. W. Choi, *Nano Lett.* **2013**, *13*, 5753 – 5761.

[9] V. T. Le, H. Kim, A. Ghosh, J. Kim, J. Chang, Q. A. Vu, D. T. Pham, J. H. Lee, S. W. Kim, Y. H. Lee, *ACS Nano* **2013**, *7*, 5940 – 5947.

[10] X. Fan, Z. Z. Chu, L. Chen, C. Zhang, F. Z. Wang, Y. W. Tang, J. L. Sun, D. C. Zou, *Appl. Phys. Lett.* **2008**, *92*, 113510.

[11] G. Z. Sun, Y. N. Zhang, L. X. Zheng, *J. Nanomater.* **2012**, 506209.

[12] G. Z. Sun, L. X. Zheng, J. Y. Zhou, Y. N. Zhang, Z. Y. Zhan, J. H. L. Pang, *Int. J. Plasticity* **2013**, *40*, 56 – 64.

[13] a) J. K. Sun, Y. H. Li, Q. Y. Peng, S. C. Hou, D. C. Zou, Y. Y. Shang, Y. B. Li, P. X. Li, Q. J. Du, Z. H. Wang, Y. Z. Xia, L. H. Xia, X. L. Li, A. Y. Cao, *ACS Nano* **2013**, *7*, 10225 – 10232; b) Z. B. Yang, H. Sun, T. Chen, L. B. Qiu, Y. F. Luo, H. S. Peng, *Angew. Chem. Int. Ed.* **2013**, *52*, 7545 – 7548; *Angew. Chem.* **2013**, *125*, 13695 – 13699; c) S. H. Aboutalebi, R. Jalili, D. Esrafilzadeh, M. Salari, Z. Gholamvand, S. A. Yamini, K. Konstantinov, R. L. Shepherd, J. Chen, S. E. Moulton, P. C. Innis, A. I. Minett, J. M. Razal, G. G. Wallace, *ACS Nano* **2014**, *8*, 2456 – 2466; d) Y. N. Meng, Y. Zhao, C. G. Hu, H. H. Cheng, Y. Hu, Z. P. Zhang, G. Q. Shi, L. T. Qu, *Adv. Mater.* **2013**, *25*, 2326 – 2331.

[14] a) A. K. Geim, K. S. Novoselov, *Nat. Mater.* **2007**, *6*, 183 – 191; b) K. S. Novoselov, V. I. Fal'ko, L. Colombo, P. R. Gellert, M. G. Schwab, K. Kim, *Nature* **2012**, *490*, 192 – 200; c) Y. X. Liu, X. C. Dong, P. Chen, *Chem. Soc. Rev.* **2012**, *41*, 2283 – 2307; d) Q. He, S. Wu, Z. Yin, H. Zhang, *Chem. Sci.* **2012**, *3*, 1764 – 1772; e) X. Huang, Z. Zeng, Z. Fan, J. Liu, H. Zhang, *Adv. Mater.* **2012**, *24*, 5979 – 6004; f) Z. Yin, J. Zhu, Q. He, X. Cao, C. Tan, H. Chen, Q. Yan, H. Zhang, *Adv. Energy Mater.* **2014**, *4*, 1300574; g) X. H. Cao, Z. Y. Yin, H. Zhang, *Energy Environ. Sci.* **2014**, *7*, 1850 – 1865; h) X. Huang, X. Qi, F. Boey, H. Zhang, *Chem. Soc. Rev.* **2012**, *41*, 666 – 686; i) G. Z. Sun, Y. Z. Pan, Z. Y. Zhan, L. X. Zheng, J. Y. Lu, J. H. L. Pang, L. Li, W. M. Huang, *J. Phys. Chem. C* **2011**, *115*, 23741 – 23744; j) G. Z. Sun, L. X. Zheng, Z. Y. Zhan, J. Y. Zhou, X. B. Liu, L. Li, *Carbon* **2014**, *68*, 748 – 754; k) H. X. Wang, Q. Wang, K. G. Zhou, H. L. Zhang, *Small* **2013**, *9*, 1266 – 1283.

[15] a) M. Chhowalla, H. S. Shin, G. Eda, L. J. Li, K. P. Loh, H. Zhang, *Nat. Chem.* **2013**, *5*, 263 – 275; b) Q. H. Wang, K. Kalantar-Zadeh, A. Kis, J. N. Coleman, M. S. Strano, *Nat. Nanotechnol.* **2012**, *7*, 699 – 712; c) X. Huang, Z. Y. Zeng, H. Zhang, *Chem. Soc. Rev.* **2013**, *42*, 1934 – 1946; d) X. Huang, C. Tan, Z. Yin, H. Zhang, *Adv. Mater.* **2014**, *26*, 2185 – 2204; e) K. G. Zhou, N. N. Mao, H. X. Wang, Y. Peng, H. L. Zhang, *Angew. Chem. Int. Ed.* **2011**, *50*, 10839 – 10842; *Angew. Chem.* **2011**, *123*, 11031 – 11034; f) W. J. Zhang, J. K. Huang, C. H. Chen, Y. H. Chang, Y. J. Cheng, L. J. Li, *Adv. Mater.* **2013**, *25*, 3456 – 3461; g) J. Pu, Y. Yomogida, K. K. Liu, L. J. Li, Y. Iwasa, T. Takenobu, *Nano Lett.* **2012**, *12*, 4013 – 4017; h) Z. Y. Yin, H. Li, H. Li, L. Jiang, Y. M. Shi, Y. H. Sun, G. Lu, Q. Zhang, X. D. Chen, H. Zhang, *ACS Nano* **2012**, *6*, 74 – 80; i) X. Huang, Z. Y. Zeng, S. Y. Bao, M. F. Wang, X. Y. Qi, Z. X. Fan, H. Zhang, *Nat. Commun.* **2013**, *4*, 1444; j) Z. Y. Zeng, C. L. Tan, X. Huang, S. Y. Bao, H. Zhang, *Energy Environ. Sci.* **2014**, *7*, 797 – 803; k) H. Li, J. Wu, Z. Y. Yin, H. Zhang, *Acc. Chem. Res.* **2014**, *47*, 1067 – 1075; l) Z. Y. Yin, X. Zhang, Y. Q. Cai, J. Z. Chen, J. I. Wong, Y. Y. Tay, J. W. Chai, J. Wu, Z. Y. Zeng, B. Zheng, H. Y. Yang, H. Zhang, *Angew. Chem. Int. Ed.* **2014**, DOI: 10.1002/anie.201402935; *Angew. Chem.* **2014**, DOI: 10.1002/ange.201402935; m) C. L. Tan, X. Y. Qi, X. Huang, J. Yang, B. Zheng, Z. F. An, R. F. Chen, J. Wei, B. Z. Tang, W. Huang, H. Zhang, *Adv. Mater.* **2014**, *26*, 1735 – 1739; n) Z. Y. Yin, B. Chen, M. Bosman, X. H. Cao, J. Z. Chen, B. Zheng, H. Zhang, *Small* **2014**, DOI: 10.1002/smll.201400124; o) C. F. Zhu, Z. Y. Zeng, H. Li, F. Li, C. H. Fan, H. Zhang, *J. Am. Chem. Soc.* **2013**, *135*, 5998 – 6001; p) Q. Y. He, Z. Y. Zeng, Z. Y. Yin, H. Li, S. X. Wu, X. Huang, H. Zhang, *Small* **2012**, *8*, 2994 – 2999.

[16] a) X. Z. Hu, Z. Xu, Z. Liu, C. Gao, *Sci. Rep.* **2013**, *3*, 2374; b) Z. Xu, C. Gao, *Nat. Commun.* **2011**, *2*, 571.

[17] X. Z. Zhou, X. Huang, X. Y. Qi, S. X. Wu, C. Xue, F. Y. C. Boey, Q. Y. Yan, P. Chen, H. Zhang, *J. Phys. Chem. C* **2009**, *113*, 10842 – 10846.

[18] a) N. N. Chai, J. Zeng, K. G. Zhou, Y. L. Xie, H. X. Wang, H. L. Zhang, C. Xu, J. X. Zhu, Q. Y. Yan, *Chem. Eur. J.* **2013**, *19*, 5948 – 5954; b) G. Eda, G. Fanchini, M. Chhowalla, *Nat. Nanotechnol.* **2008**, *3*, 270 – 274; c) X. C. Dong, C. Y. Su, W. J. Zhang, J. W. Zhao, Q. D. Ling, W. Huang, P. Chen, L. J. Li, *Phys. Chem. Chem. Phys.* **2010**, *12*, 2164 – 2169.

[19] a) S. F. Pei, J. P. Zhao, J. H. Du, W. C. Ren, H. M. Cheng, *Carbon* **2010**, *48*, 4466 – 4474; b) I. K. Moon, J. Lee, R. S. Ruoff, H. Lee, *Nat. Commun.* **2010**, *1*, 73.

[20] W. J. Yuan, Y. Zhou, Y. R. Li, C. Li, H. L. Peng, J. Zhang, Z. F. Liu, L. M. Dai, G. Q. Shi, *Sci. Rep.* **2013**, *3*, 2248.

[21] Z. Y. Zeng, Z. Y. Yin, X. Huang, H. Li, Q. Y. He, G. Lu, F. Boey, H. Zhang, *Angew. Chem. Int. Ed.* **2011**, *50*, 11093 – 11097; *Angew. Chem.* **2011**, *123*, 11289 – 11293.

[22] Y. H. Chang, C. T. Lin, T. Y. Chen, C. L. Hsu, Y. H. Lee, W. J. Zhang, K. H. Wei, L. J. Li, *Adv. Mater.* **2013**, *25*, 756 – 760.

[23] T. Stephenson, Z. Li, B. Olsen, D. Mitlin, *Energy Environ. Sci.* **2014**, *7*, 209 – 231.

[24] X. Gu, W. Cui, H. Li, Z. W. Wu, Z. Y. Zeng, S. T. Lee, H. Zhang, B. Q. Sun, *Adv. Energy Mater.* **2013**, *3*, 1262 – 1268.

[25] L. J. Cao, S. B. Yang, W. Gao, Z. Liu, Y. J. Gong, L. L. Ma, G. Shi, S. D. Lei, Y. H. Zhang, S. T. Zhang, R. Vajtai, P. M. Ajayan, *Small* **2013**, *9*, 2905 – 2910.
[26] a) P. Simon, Y. Gogotsi, *Nat. Mater.* **2008**, *7*, 845 – 854; b) J. J. Yoo, K. Balakrishnan, J. S. Huang, V. Meunier, B. G. Sumpter, A. Srivastava, M. Conway, A. L. M. Reddy, J. Yu, R. Vajtai, P. M. Ajayan, *Nano Lett.* **2011**, *11*, 1423 – 1427; c) M. D. Stoller, S. J. Park, Y. W. Zhu, J. H. An, R. S. Ruoff, *Nano Lett.* **2008**, *8*, 3498 – 3502.
[27] P. H. Yang, Y. Ding, Z. Y. Lin, Z. W. Chen, Y. Z. Li, P. F. Qiang, M. Ebrahimi, W. J. Mai, C. P. Wong, Z. L. Wang, *Nano Lett.* **2014**, *14*, 731 – 736.
[28] J. Bae, Y. J. Park, M. Lee, S. N. Cha, Y. J. Choi, C. S. Lee, J. M. Kim, Z. L. Wang, *Adv. Mater.* **2011**, *23*, 3446 – 3449.
[29] J. Ren, L. Li, C. Chen, X. L. Chen, Z. B. Cai, L. B. Qiu, Y. G. Wang, X. R. Zhu, H. S. Peng, *Adv. Mater.* **2013**, *25*, 1155 – 1159.
[30] X. L. Chen, L. B. Qiu, J. Ren, G. Z. Guan, H. J. Lin, Z. T. Zhang, P. N. Chen, Y. G. Wang, H. S. Peng, *Adv. Mater.* **2013**, *25*, 6436 – 6441.
[31] a) F. Tristán-López, A. Morelos-Gómez, S. M. Vega-Diaz, M. L. Garcia-Betancourt, N. Perea-López, A. L. Elías, H. Muramatsu, R. Cruz-Silva, S. Tsuruoka, Y. A. Kim, T. Hayahsi, K. Kaneko, M. Endo, M. Terrones, *ACS Nano* **2013**, *7*, 10788 – 10798; b) Y. Wang, Y. P. Wu, Y. Huang, F. Zhang, X. Yang, Y. F. Ma, Y. S. Chen, *J. Phys. Chem. C* **2011**, *115*, 23192 – 23197.
[32] a) I. Y. Kim, S. Park, H. Kim, S. Park, R. S. Ruoff, S.-J. Hwang, *Adv. Funct. Mater.* **2014**, *24*, 2288 – 2294; b) J. Li, X. Cheng, J. Sun, C. Brand, A. Shashurin, M. Reeves, M. Keidar, *J. Appl. Phys.* **2014**, *115*, 164301.
[33] a) K. Chang, W. X. Chen, *ACS Nano* **2011**, *5*, 4720 – 4728; b) S. B. Yang, Y. J. Gong, Z. Liu, L. Zhan, D. P. Hashim, L. L. Ma, R. Vajtai, P. M. Ajayan, *Nano Lett.* **2013**, *13*, 1596 – 1601.

